2016

Investigations on Performance of an Auto-Cascade Absorption Refrigeration System Operating with Mixed Refrigerants

Shengjian Le
qtxz1234567890@126.com

Qin Wang
wangqin@zju.edu.cn

Dahong Li

Xiaohong Han

Guangming Chen

INVESTIGATIONS ON THE PERFORMANCE OF AN AUTO-CASCADE ABSORPTION REFRIGERATION SYSTEM OPERATING WITH MIXED REFRIGERANTS

Shengjian LE, Qin WANG*, Dahong LI, Xiaohong HAN, Guangming CHEN

Institute of Refrigeration and Cryogenics, State Key Laboratory of Clean Energy Utilization, Zhejiang University, Hangzhou 310027, China

+86 13989489559 wangqin@zju.edu.cn

ABSTRACT

Waste heat can be well utilized in absorption refrigeration systems. The auto-cascade absorption refrigeration system could reach a lower temperature than traditional one because the non-azeotropic mixed refrigerants were used. In this paper, performances of an auto-cascade absorption refrigeration with R23/R134a/DMF (Dimethylformamide) as the working substance was analysed. Theoretical analysing results showed that, to some extent, the *COP* could be increased when the low pressure of the system decreased or the high pressure increased. The reasonable high pressure was the high turning point pressure, and reasonable low pressure was the low turning point pressure. The *COP* of the system monotonously increased with the increase of the mole fraction of R23. The lowest R23 mole fraction one should be the most promising.

1. INTRODUCTION

The absorption refrigerator is one of heat driven refrigerating devices, which takes advantages of solution properties to obtain low temperatures. Industrial waste heat, solar heat and geothermal heat were suitable to drive absorption refrigerators, therefore, absorption refrigerators were attracted more and more attentions nowadays. Traditional LiBr/H_2O or NH_3/H_2O absorption refrigerators had been widely applied in industries and daily life, but they were limited by their relatively high refrigeration temperatures. Huge quantities of waste heat were released in oil refining industries and refrigeration temperature below -50 ℃ was demanded during the process of recovery of LPG. Some research data indicated that recovery of 1000kg fuel gas consumed 65kWh refrigeration capacity (Bruno and Guxens, 2002). Under the circumstances, traditional NH_3/H_2O absorption refrigerators had to add additional devices and complex pipe arrangement to multistage absorption form to reach that low temperature.

Fatouh and Srinivasa Murthy (1995) carried researches on the properties of R22 and inorganic solutions, which showed advantages over traditional working substances and were suitable for lower generation temperature between 75 ℃ and 95 ℃.

Chen *et al.* (1998) proposed non-azeotropic mixed refrigerant R22/R142b in the traditional absorption refrigeration system to replace R22 when DMF (N, N-dimethylformamide) was selected as the absorbent in 1998. Furthermore, they proposed R32/R134a as the mixed refrigerant (Chen *et al.*, 1999a) and found similar system performances can be obtained from test results (Chen *et al.*, 1999b). In 2010, Gao *et al.* (2010) analysed the feasibility of replacing R22 with R32/R227ea in the traditional absorption system. The results also showed that similar system performances can be obtained when DMF was used as the absorbent.

In 2002, Chen (2002) introduced the auto-cascade module into the traditional absorption refrigeration system to obtain a lower refrigerating temperature. The followed up experiments showed promising system performances: the lowest refrigerating temperature was -47.2 ℃ when the generation temperature was 157 ℃ (Chen and He, 2007). The new system was named as the auto-cascade absorption refrigeration system.

As the operation mechanism of the new system is far more complicated than that of the traditional one, theoretical analyses on the performance of the new system has not been investigated systematically so far. This paper proposed a new approach to analyse and optimize the performance of the new system and showed how pressure and refrigerants concentration work in the system(Gao, 2010), which can be a useful guide for the future experiment researches.

2. THEORETICAL MODEL

The key characteristic of the auto-cascade absorption refrigeration system was that the non-azeotropic mixed refrigerant was applied as working substances, in which the non-azeotropic mixed refrigerant went through temperature-changing phase change processes. Thus at the exits of the evaporator and condenser, the mixed refrigerants still remained in the two-phase states, which demanded a recuperator with a large area to liquefy the mixed refrigerants in the high pressure side before entering the expansion valve, in order to obtain a low refrigerating temperature. The flow chart of the auto-cascade absorption refrigeration system was shown in Figure 1.

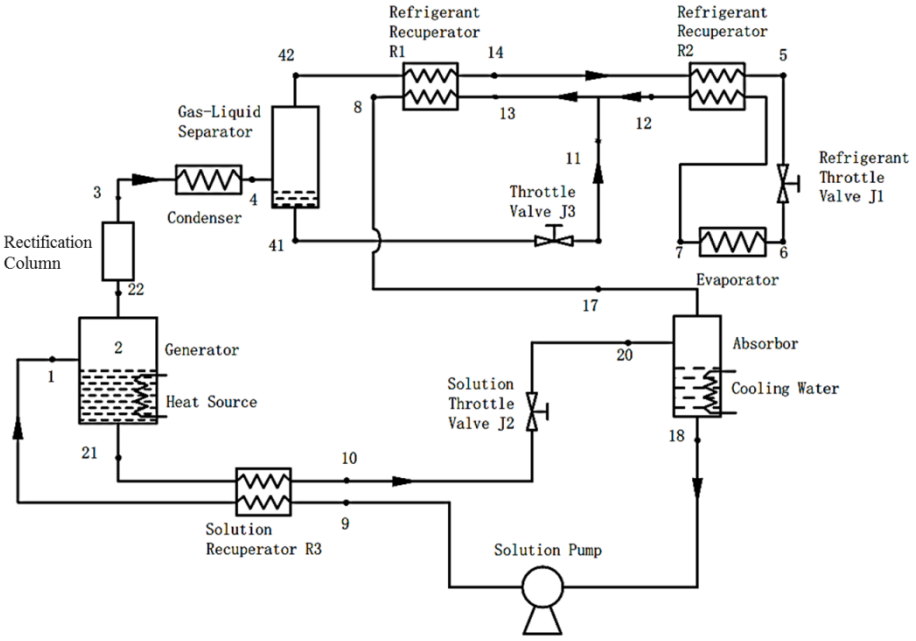

Figure 1. Flow chart of the auto-cascade absorption refrigeration system

2.1. Assumption

(1) The generating temperature T_G, surroundings temperature T_H and refrigerating temperature T_L were specified.
(2) The mole fraction of rich solution was specified as well as the mole fraction of DMF at the exit of rectification column point 3.
(3) The high pressure and low pressure of the system were specified. The pressure losses in the heat exchangers and rectifier were neglected.
(4) The pinch point temperature differences of the condenser $\Delta T_{C,min}$ and evaporator $\Delta T_{E,min}$ occurred at the cold end of the condenser and the hot end of the evaporator, respectively.
(5) The pinch point temperature differences of the refrigerant recuporator R1, R2 and solution recuperator R3 were $\Delta T_{R1,min}$, $\Delta T_{R2,min}$ and $\Delta T_{R3,min}$ respectively. All of the pinch points occurred at the cold or hot end of the recuperators.
(6) The pinch point temperature difference of the absorber $\Delta T_{A,min}$ occurred at the exit of absorber.
(7) Refrigerant recuperators, solution recuperator and throttle valves were adiabatic.

2.2. Thermodynamic Model

The mass conservation and energy conservation equations of all parts in the auto-cascade absorption refrigeration system were listed as follows.

(1) Generator

$$Q_G = m_{22}h_{22} + m_{21}h_{21} - m_1h_1 \quad (1)$$
$$m_1 = m_{22} + m_{21} \quad (2)$$
$$m_1z_{1,i} = m_{22}z_{22,i} + m_{21}z_{21,i} \quad (3)$$

where m was the mole flow rate of the working substance [mol $\cdot s^{-1}$], h was the specific enthalpy [J $\cdot mol^{-1}$], Q_G was the heat input in the generator [W], z was the mole fraction of the component, the first subscript denoted the state point in the cycle, the second subscript i denoted the i_{th} component of the mixture R23/R134a/DMF.

(2) Rectifier

$$m_{22} = m_3 + m_L \quad (4)$$
$$m_{22}z_{22,i} = m_3z_{3,i} + m_Lz_{21,i} \quad (5)$$
$$m_{22}h_{22} = m_3h_3 + m_Lh_L + Q_D \quad (6)$$

where Q_D was the rectifying heat capacity [W], subscript L denoted the backflow to the generator.

(3) Absorber

$$Q_A = m_{20}h_{20} + m_{17}h_{17} - m_{18}h_{18} \quad (7)$$
$$m_{18} = m_{20} + m_{17} \quad (8)$$
$$m_{18}z_{18,i} = m_{20}z_{20,i} + m_{17}z_{17,i} \quad (9)$$

where Q_A denoted the absorbing heat released to the surroundings [W].

(4) Condenser

$$Q_C = m_4(h_4 - h_3) \quad (10)$$

where Q_C denoted the condensing heat released to the surroundings.

(5) Gas-liquid separator

The compositions of R23/R134a/DMF vapour and weak solution in the separator could be determined by the vapour-liquid equilibrium.

$$m_4 = m_{42} + m_{41} \quad (11)$$
$$m_4z_{4,i} = m_{42}z_{42,i} + m_{41}z_{41,i} \quad (12)$$
$$m_4h_4 = m_{42}h_{42} + m_{41}h_{41} \quad (13)$$

(6) Recuperators

Two refrigerant recuperators were treated as a whole one.

$$m_{42}(h_5 - h_{42}) = m_7(h_8 - h_7) \quad (14)$$

Solution recuperator was defined as:

$$m_{21}(h_{21} - h_{10}) = m_9(h_9 - h_1) \quad (15)$$

(7) Throttle valves

The throttle valve at the bottom of the separator:

$$m_{41}h_{41} = m_{11}h_{11} \quad (16)$$

The refrigerant throttle valve:

$$m_5h_5 = m_6h_6 \quad (17)$$

The solution throttle valve:

$$m_{10}h_{10} = m_{20}h_{20} \tag{18}$$

(8) Evaporator

$$m_7(h_7 - h_5) = Q_E \tag{19}$$

where Q_E denoted the refrigerating capacity [W].
(9) Solution pump
Compared to the amount of heat input into the system, the work consumed by the solution pump was small which was neglected.
(10) Coefficient of performance

$$COP = Q_E/Q_G \tag{20}$$

COP could also be expressed as the following form:

$$COP = (h_7 - h_5)/\big(f(h_{21} - h_1) + (h_{22} - h_{21})\big) \tag{21}$$
$$COP = (h_8 - h_{42})/\big(f(h_{21} - h_1) + (h_{22} - h_{21})\big) \tag{22}$$

where circulating ratio:

$$f = m_1/m_{22} \tag{23}$$

2.3. Calculation Of Properties of the Mixture

Modified Patel-Teja equation was applied in this paper to calculate the enthalpy, entropy and phase equilibrium of the mixed refrigerants. The interaction parameters of each pair among R23, R134a and DMF were fitted from literatures (Han *et al.*, 2011, Gao *et al.*, 2012).

3. PERFORMANCE ANALYSIS AND OPTIMIZATION

In calculations, the generation temperature T_G=140 ℃, surroundings temperature T_H=20 ℃, refrigerating temperature T_L=-50 ℃, the mole fraction of DMF at point 3 $z_{3,3}$=0.03. The pinch point temperature difference $\Delta T_{R1,min}$=$\Delta T_{R2,min}$=$\Delta T_{C,min}$=$\Delta T_{E,min}$=5 ℃, $\Delta T_{A,min}$=10 ℃. The flow rate at point 2 was set to be 1mol/s.

3.1. Optimization Of Pressures

The high and low pressures of the auto-cascade absorption refrigeration system were not only related with condensation temperature and evaporation temperature, but also associated with the generation temperature, absorption temperature and the temperature distribution of mixed refrigerants in recuperators attribute to the introduce of the high non-azeotropic refrigerant. Hence, the high pressure and low pressure were treated as two important design parameters in simulations.

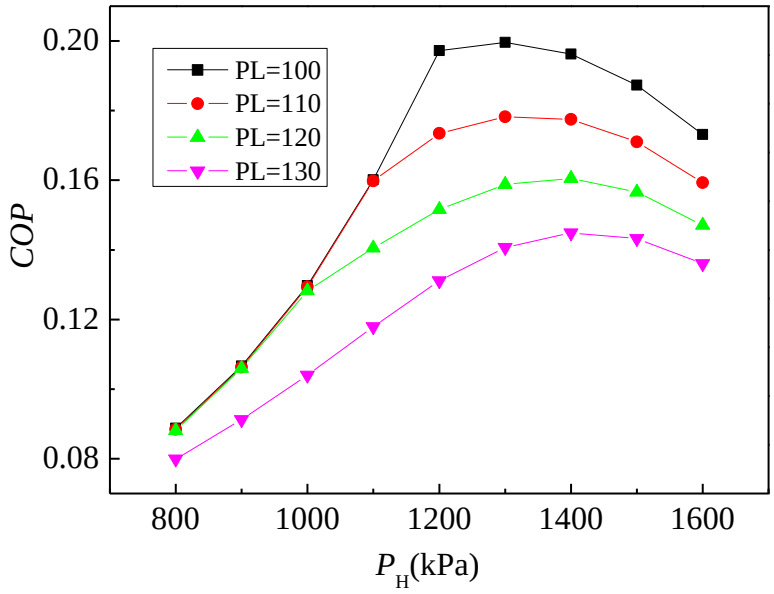

Figure 2. The variation of *COP* with the high pressure P_H ($z_{1,1}$=0.2, $z_{1,3}$=0.6)

From figure 2, it can be seen that a peak *COP* occurred with the increase of the high pressure at each low pressure. Hence, the corresponding high pressure can be selected as the reasonable high pressure at certain low pressure.

It can also be noted from Figure 2 that *COP* monotonically increased with the decrease of the low pressure at certain high pressure. In order to see clearly the variation of *COP* with the low pressure, the abscissa was reset as the low pressure P_L as showed in Figure 3.

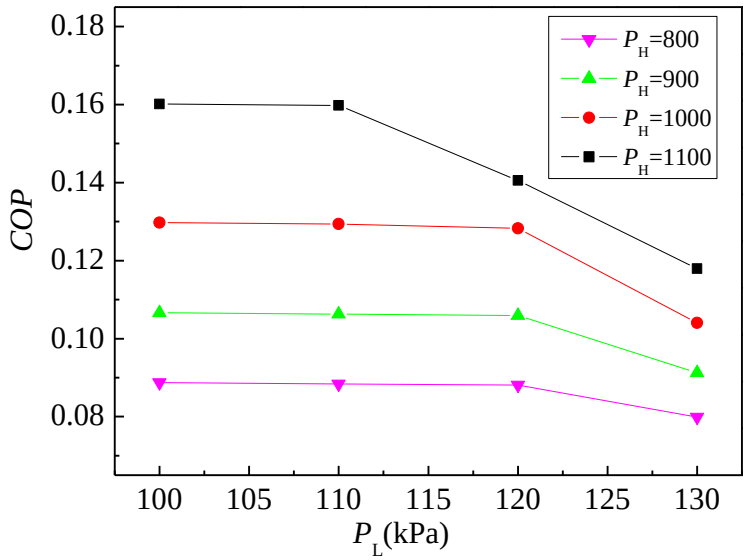

Figure 3. The variation of *COP* with the low pressure P_L ($z_{1,1}$=0.2, $z_{1,3}$=0.6)

From figure 3, it can be seen that *COP* increased with the decrease of the low pressure at the specified high pressure and there existed a turning point along the line. When the low pressure was larger than the turning point low pressure *COP* increased obviously, but when the low pressure was smaller than the turning point low pressure *COP* increased very slightly. Hence, the turning point low pressure can be selected as the reasonable low pressure at certain high pressure, because the extreme low pressure deteriorated the performance of the absorber and increased the power consumption of the solution pump.

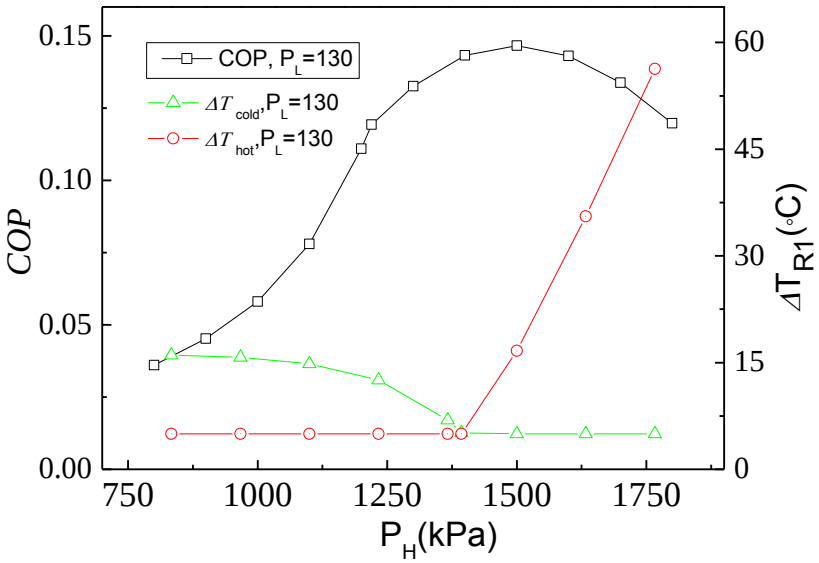

Figure 4. The variation of *COP*, ΔT_{hot}, ΔT_{cold} with the high pressure ($z_{1,1}$=0.2, $z_{1,3}$=0.6, P_L=130kPa)

The variations of *COP* with the high pressure and low pressure discussed above have been found in other mole fractions of R23/R134a/DMF solutions. It can also be found that the temperature differences at the hot end of the refrigerant recuperator R1 and at the cold end of the refrigerant recuperator R2 varied regularly with the pressures.

From figure 4, it can be found that the temperature differences at the hot end of R1 and at the cold end of R2 were both approximately equal to the pinch point temperature differences of R1 and R2 respectively, namely, $\Delta T_{cold}=\Delta T_{hot}=\Delta T_{min}$, when *COP* occurred a peak value with the increase of high pressure. In other words, at a specified low pressure the pinch point temperature difference transferred from the hot end of R1 to the cold end of R2 when the high pressure increased. Because the heat demanded for the generator varied slightly, hence, the variation of *COP* was mainly determined by the cooling capacity change with the increase of the high pressure. After the transfer of the pinch point to the cold end of R2, the specific enthalpy difference between state points 5 and 7 increased slightly, but the refrigerant flow rate decreased from the top outlet of the gas-liquid separator when the high pressure increased. These factors can account for the occurrence of the peak value of *COP* in Figure 4.

Figure 5 also showed that the temperature differences at the cold end of R2 and at the hot end of R1 were both approximately equal to the pinch point temperature differences of R1 and R2 respectively, namely $\Delta T_{cold}=\Delta T_{hot}=\Delta T_{min}$, *COP* occurred a turning point with the decrease of the low pressure.

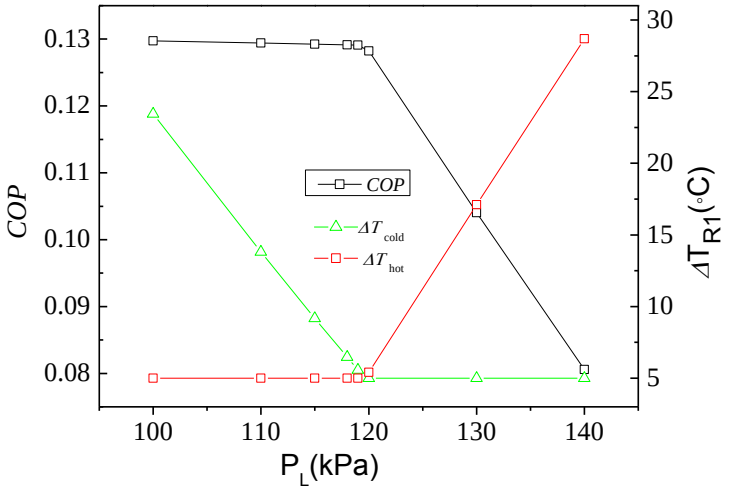

Figure 5. The variation of *COP*, ΔT_{hot}, ΔT_{cold} with the low pressure ($z_{1,1}$=0.2, $z_{1,3}$=0.6, P_H=1000kPa)

From the above analyses, we knew that the low and high pressures at the turning points should be the reasonable low and high pressures for the specified mole fractions of the solution. In this paper, the reasonable low pressure was specified as 100kPa. The peak value of *COP* at the reasonable low and high pressures for the specified mole fractions was defined as the COP_{opt}.

3.2. Optimization Of Mole Fractions

According to the pressure optimizing method in previous section, COP_{opt} of different mole fractions could be obtained. Figure 6 showed the variations of COP_{opt} and refrigerating capacity Q_E with the mole fraction of R23 when the mole fractions of DMF $z_{1,3}$ were set to be 50%, 60% and 70%.

From figure 6, it can be seen that Q_E and COP_{opt} both increase monotonically with the increase of R23 for the specified mole fraction of DMF $z_{1,3}$,. The maximum COP_{opt} for different mole fractions of DMF were almost same, but the corresponding high pressures to COP_{opt} were different. The larger mole fraction of DMF, the higher the corresponding high pressure was.

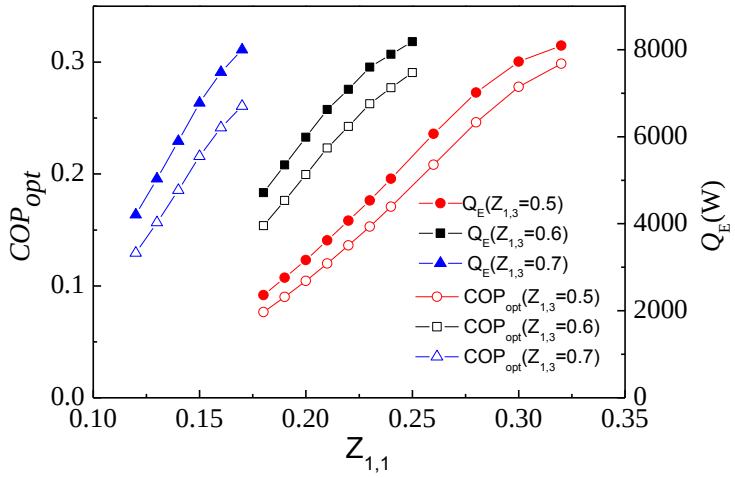

Figure 6. The variation of COP_{opt} and Q_E with the fraction of R23 (T_G= 140 ℃, T_H= 20 ℃, T_L= -50 ℃, $z_{3,3}$=0.03)

4. CONCLUSION

The performance of an auto-cascade absorption refrigeration cycle operated with non-azeotropic refrigerant R23/R134a/DMF was investigated in this paper by a new approach. The analysis results showed that:

(1) At a specified low pressure, *COP* increased at first and then decreased with the increase of the high pressure. The high pressure corresponding to the peak *COP* should be the reasonable high pressure.

(2) At a specified high pressure, *COP* was obviously increased with the decrease of low pressure within a certain range. The turning point low pressure should be the reasonable low pressure.

(3) When the temperature differences at the cold end of R2 and at the hot end of R1 were both approximately equal to the pinch point temperature differences of R1 and R2 respectively, the peak value or the turning point occurred.

(4) When the mole fraction of DMF was specified, refrigerating capacity Q_E and COP_{opt} both increased monotonically with the increase of the mole fraction of R23. But the maximum COP_{opt} were almost the same for different mole fractions of DMF. As the high pressure corresponding to the maximum COP_{opt} for the low mole fraction of DMF solution was lower than that of high mole fraction of DMF solutions, the low mole fraction one should be the most promising.

NOMENCLATURE

COP	coefficient of performance	(–)
T	temperature	℃
ΔT	temperature difference	℃
Q	heat load	W
h	enthalpy	$J \cdot mol^{-1}$
m	mole flow rate	$mol \cdot s^{-1}$
z	mole fraction of components	(–)
f	circulating ratio	(–)
P	pressure	kPa

Subscript

G	generator
H	high
L	low
R1	recuperator 1
R2	recuperator 2
R3	recuperator 3
C	condenser
E	evaperator
A	absorber
D	rectifier
hot	hot end
cold	cold end
opt	optimum

REFERENCES

Bruno JC, Guxens S. 2002, Efficiency improvement in oil refining process using absorption refrigeration plants driven by waste heat, *ISHPC'02, Proceedings of the International Sorption Heat Pump Conference*, 111-116.

Chen G. 2002, *Absorption Refrigeration Device Used for Deep Freezing*, ZL02110940.0

Chen S, Chen G, Zheng F, Zhang H. 1999, Operation Characteristics of Absorption Refrigeration Using Alternative Working Fluids, *Cryogenics*. 112(6): 22-30.

Chen G, He Y. 2007, Experimental Study on an Absorption Refrigeration Cycle, *Journal of Thermal Science*. 47(3): 294-299.

Chen G, Yin Z, Wang J, Zheng F, Jiang H. 1998, The Characteristics of a Absorption System with Azeotropic Refrigerant Mixture Refrigerant, *Journal of Refrigeration*. 1: 1-5.

Chen S, Zheng F, Wang J, Chen G. 1999, Replacement Refrigerant HCFC22 for Absorption Refrigeration Features, *Journal of Engineering Thermophysics*. 20(4): 410-412.

Gao W, Zhao X, Liu Z. 2010, Calculation of HFC32+HFC227ea/DMF Absorption Refrigeration Cycle, *Journal of Engineering Thermophysics*. 31(4): 545-548.

Gao Z, Xu Y, Li P, Cui X, Han X, Wang Q, Chen G. 2012, Solubility of Refrigerant Trifluoromethane in n,n-Dimethyl Formamide in the Temperature Range from 283.15K to 363.15K, *Int. J. Refrig*. 35(5): 1372-1376.

Gao X, Theoretical and Experimental Study on Mixed Refrigerants Absorption Refrigeration System Used for Deep Freezing, Zhejiang University, 2010.

Fatouh M, Srinivasa Murthy S. 1995, Performance of an HCFC22-based vapour absorption refrigeration system, *Int. J. Refrig*. 18(7): 465-476.

Han X, Gao Z, Xu Y, Qiu Y, Min X, Cui X, Chen G. 2011, Solubility of Refrigerant 1,1,1,2-Tetrafluoroethane in the N,N-Dimethyl Formamide in the Temperature Range from 263.15K to 363.15K, *Chem. Eng. Data.* 56(5): 1821-1826.